Research Article

Event-related potential arithmetic to analyze offset potentials from conscious mice

Jamie A. O'Reilly [a, b, c]

[a] College of Biomedical Engineering, Rangsit University, Pathumthani, Thailand.

[b] Department of Biomedical Engineering, University of Strathclyde, Glasgow, UK.

[c] Strathclyde Institute of Pharmacy and Biomedical Science, University of Strathclyde, Glasgow, UK.

Present Address:

College of Biomedical Engineering, Rangsit University
52/347 Muang-Ake, Phaholyothin Road,
Pathum Thani 12000, Thailand
Phone: +66(0)64 783 4785
E-mail: jamie.o@rsu.ac.th

Declarations of interest: none

Abstract

Background This paper presents a method for isolating time-dependent event-related potential (ERP) components which are superimposed on the gross ERP waveform. The experimental data that inspired this approach was recorded from the auditory cortex of conscious laboratory mice in response to presentation of ten different duration pure-tone auditory stimuli.

New Method The grand-average ERP for each individual stimulus displayed a relatively low amplitude deflection following stimulus offset. In order to isolate this component for analysis, a series of simple arithmetic operations were performed, involving averaging of multiple stimuli ERPs and subtracting this from each individual ERP.

Results Offset potentials were isolated and quantified. Peak latency was determined by auditory stimulus duration; peak amplitude did not reach the threshold for statistical significance, over the range of durations tested.

Comparison with Existing Method(s) To the best of my knowledge there are no alternative methods for isolating offset potentials from the gross ERP waveform at present. This novel approach may introduce less subjective bias to analyses than manually selecting measurement windows and performing custom baseline corrections.

Conclusions A similar method may be applied to other human or non-human datasets to identify and characterize time-dependent sensory-cognitive processes obscured by gross waveform morphology.

Keywords ERP analysis, ERP arithmetic, ERP component isolation, ERP operations, offset response

Funding This research was supported in part by the UK EPSRC (EP/L015595/1)

Declarations of interest None

1. Introduction

The event-related potential (ERP) technique was pioneered in 1939 by Pauline and Hallowell Davis (Davis et al., 1939). With the development of digital computers this led to a revolution in electroencephalography (EEG) research, which until then been hampered by a poor signal-to-noise ratio (SNR). High temporal precision of EEG relative to other functional neuroimaging modalities (e.g. fMRI) ensures it remains useful today for analyzing brain responses to discrete experimental events, such as sensory stimulation or subject actions. However, the low amplitude scalp potentials measured are oftentimes swamped by electromagnetic interference (EMI), both from biological and non-biological sources. To improve the SNR, EEG data is recorded across multiple trials where the same event (stimulus or action) is repeated. The recording is then segmented around each event. These segments are checked for contaminant EMI, usually with an artifact rejection threshold, and offending segments are discarded. The resulting 'clean' segments are averaged together to produce the ERP. This effectively reduces electrical potentials not time-locked to the event, leaving a clearer representation of the average neural response evoked by said event.

This technique has been widely deployed in the examination of sensory and cognitive neuroscience (Luck and Kappenman, 2011), and beyond human studies has been applied broadly to examine the neurophysiology of animal models (O'Connor and Starr, 1985; Ruusuvirta et al., 1998; Woodman et al., 2007). In his handbook, Steven J. Luck (Luck, 2014) describes the ERP methodology, including the ability to apply various mathematical operations to manipulate waveforms. Subtraction is perhaps the most well-known of these operations, beyond the averaging process normally involved in computing the ERP, producing a difference-wave, most commonly associated with mismatch negativity (MMN) evoked during an oddball paradigm (Näätänen et al., 2012). Otherwise, there are few examples of ERP arithmetic applied in the literature (Luck and Kappenman, 2011).

Rodents are the most commonly used laboratory animal for medical research. As such, there are numerous examples of ERP studies in rodents. This paper presents an analysis of duration many-standards paradigm data recorded from mice (Harms et al., 2014). This was performed as part of a larger study examining auditory electrophysiology in mouse models of neuropsychiatric disease; the data presented here are stored in an open-access repository (O'Reilly, 2018, 2017). Different duration stimuli were played to mice while recording bioelectric activity from the auditory cortex. Resulting ERP waveforms displayed a component synchronized with sound cessation of relatively low-amplitude compared with the much larger amplitude ERP peaks occurring at stimulus onset. A novel application of ERP arithmetic was necessitated by the presence of these deflections occurring at the terminus of auditory stimulation. Although stimulus-off potentials have previously been observed from anaesthetized rats (Nakamura et al., 2011), to the best of my knowledge, in the published literature no attempt has been made to separate them from the overall ERP. This presented a challenge, for which ERP arithmetic provided a solution. In this paper, basic principles of arithmetic (addition, subtraction and division) are applied to isolate and analyze offset potentials from the ERPs to different duration auditory stimuli. This approach may be taken in other controlled circumstances were temporally precise events are recorded from animals or human subjects.

2. Material and methods

2.1 Animals

Twenty laboratory mice (>99.999% C57BL/6J genetics) were used in this experiment. These were bred in-house at the University of Strathclyde's Biological Procedures Unit (BPU). This group consisted of 9 males and 11 females aged 29-37 weeks ($\bar{x}$ = 32.4). Males weighed from 27.8 to 36 g ($\bar{x}$ = 33g) and females from 23.8 to 26.3 g ($\bar{x}$ = 25g). Different genders were housed separately to restrict the breeding program. They were housed in groups of two or more in an atmospherically controlled holding room at 21°C (±1°C), 55% relative humidity (±10%) with a 12hr light cycle from 0700 to 1900 GMT. Standard CRM pelleted rodent chow (Special Diets Services, UK) and water was freely available inside each home-cage. Additional chocolate treat was given mice for several days after undergoing surgery. High-top home-cages were used to mitigate post-surgical insults from head-stage catching. Levels of auditory stimuli employed in this experiment were chosen to exceed the predicted hearing threshold of C57BL/6J laboratory mice of this age range (Ison et al., 2007). Electrophysiological recordings were made from conscious mice following recovery from electrode implantation surgery. All of the procedures concerning animals were approved by the Animal Welfare and Ethical Review Body at University of Strathclyde and performed in accordance with the UK Animals (Scientific Procedures) Act 1986.

2.2 Surgery

Isoflurane and oxygen 5:1% (Fisher Scientific, UK) were used to induce anesthesia. After induction, isoflurane concentration was decreased to 1.5% for maintenance. Anesthetic depth was verified continuously by confirming absent response to painful stimuli (tail and toe pinch) and eye-blink reflexes. Animals were fixed into a stereotactic frame for rodents (David Kopf Instruments, USA) to perform electrode implantation. They were placed on a heating pad (35°C) to maintain their body temperature. The surgical area was cleaned using Tamodine (Vetark, UK) and rinsed with sterile saline. Lidocaine (2%, 0.1 – 0.2 ml/kg) was then injected subcutaneously to provide local analgesia to the incision site. An anterior-to-posterior incision on top of the head was performed and a thin underlying layer of soft tissue was bluntly dissected to expose the skull. Hydrogen peroxide 3% (Fisher Scientific, UK) was applied to the surgical site for antisepsis. Electrode implantation sites above the primary auditory cortices (2.2 mm caudal and 3.8 mm lateral relative to Bregma (Paxinos and Franklin, 2004)) were plotted using a stereotactic manipulator. A dental drill was used to make shallow burr holes and skull-screw electrodes (ø = 1 mm; Royem Scientific, UK) were implanted, including a single ground electrode above the cerebellum. Electrodes were positioned at the surface of the cortex. They were wired and soldered to a custom head-stage connector (SDL-12-G-10; Samtec, USA), glued to the skull with dental acrylic (Simplex Rapid; Associated Dental Products, UK). Figure 1 illustrates the layout of the implanted components following surgery. Carprofen 5 mg/kg (Fisher Scientific, UK) was injected subcutaneously in the lateral inferior abdomen for postoperative analgesia. The surgical area was re-cleaned with Tamodine and rinsed with sterile saline before reviving animals. Aseptic surgical technique was applied throughout and mice were monitored during recovery for at least five days post-surgery before conducting electrophysiological recordings. No postoperative complications were observed.

2.3 Equipment

Animals were placed inside a customized recording chamber during experiments. This was electrically shielded and acoustically controlled using sound-attenuating foam. Background noise was measured at <55 dB using a sound meter (Model 33-2055; Radioshack, USA). Within the chamber mice were held in a perforated restraining tube commonly used for pre-pulse inhibition experiments. Front- and rear-facing loudspeakers were used to deliver auditory stimulation; to reduce the impact of mouse orientation within the tube on incident stimulus properties. These were each calibrated (A-weighted) to the approximate position of the animal. The head-stage connector was tethered to the recording system (Figure 2). Epidural potentials were acquired with a sampling frequency of 1 kHz and band-pass filtered between 0.1-500 Hz using a unipolar arrangement amplifier board (RHD2132; Intan Technologies, USA) connected to an FPGA board (RHD Evaluation System; Intan Technologies, USA) via a computer USB port. Open source electrophysiology software (open-ephys.org) provided visualization and data storage functions. Custom Matlab (Mathworks, USA) scripts were designed to generate and deliver auditory stimuli and synchronization signals via a USB I/O device (USB-6255; National Instruments, USA).

2.4 Auditory Paradigm

Ten different duration stimuli (50, 75, 100, 125, 150, 175, 200, 225, 250, and 275 ms) were presented one hundred times each, in pseudorandom order, with an inter-stimulus interval of 450 ms. These were all 10 kHz monophonic pure-tone sine waves, delivered at 80 dB sound pressure level, with instantaneous rise/fall times. In mismatch negativity research this is known as a many-standards control paradigm (Harms et al., 2014).

2.5 Data Analysis

Event-related potentials were computed for each of the ten different duration stimuli. Electro-encephalographic data was segmented into epochs of 50 ms pre-stimulus- to 350 ms post-stimulus-onset. Pre-stimulus baseline correction was applied. Segments containing electrical interference exceeding 500 µV were automatically rejected. The remaining segments were then averaged to produce an ERP for each stimulus, equating to ten per animal, which were further combined to produce study grand-average ERPs. For quantification of peak amplitude and latency, measurements were taken from the ERPs recorded from each animal. This analysis was performed offline using the Python library, MNE (Gramfort et al., 2013).

Simple arithmetic operations were performed on ERPs in order to isolate waveform deflections observed to coincide with stimuli offset times. Namely, the average ERP as a function of time [$\overline{ERP}(t)$] was produced by summing each individual ERP as a function of time [$ERP_x(t)$] and dividing by *n* (1). In this experiment, formula (1) defines the average ERP across all duration stimuli, calculated for each animal individually. In order to isolate the stimulus-off component, this average ERP was then subtracted from each individual ERP to reveal the isolated ERP [$ERP_{x_{iso}}(t)$] (2).

$$\overline{ERP}(t) = \frac{1}{n}\sum_{x=1}^{n} ERP_x(t) \quad (1)$$

$$ERP_{x_{iso}}(t) = ERP_x(t) - \overline{ERP}(t) \quad (2)$$

Where *n* is the total number of individual ERPs (ten in this case), *x* indexes each individual ERP, and *t* is the epoch time point (running from 50 ms pre-stimulus to 350 ms post-stimulus onset). The application of these operations to separate low amplitude deflections time-locked to stimulus offset from the gross ERP waveform, is illustrated in Figure 4.

Peak latency and amplitude measurements were taken from isolated ERP waveforms. A measurement window of 0-350 ms post stimulus onset was used to measure peak latency, while peak amplitude was measured over 0-50 ms post stimulus offset. Linear mixed-effects models were computed to quantify correlation of the aforementioned with stimulus duration, taking into account multiple measures from individual animals (Laird et al., n.d.). Repeated measures analysis of variance (rmANOVA) were also performed on these data. The Bonferroni adjustment was applied to correct for ten within-subject repeated measures (i.e. 10 ERP measurements per animal), therefore the threshold for rejecting the null hypothesis was set to 0.005. These statistical analyses were performed using R (Team, 2018).

3. Results

Grand-average auditory ERP waveforms from each duration stimulus are plotted in Figure 3. From this viewpoint it is difficult to discriminate between the ERPs, and they appear qualitatively similar. However, when these waveforms are overlaid on top of one another, as in Figure 4a, a distinct feature becomes apparent. There is a relatively low amplitude positive deflection occurring immediately after stimuli offset times. The first step towards isolating these waveform features was to produce the average ERP (1) plotted in Figure 4b. This was then subtracted from each individual ERP in turn to isolate the stimulus offset potentials (2) shown in Figure 4c. This demonstrates how performing simple arithmetic operations on ERPs may be used to effectively isolate waveform features of interest, which in this case were stimuli offset potentials.

Peak latency and amplitude measurements from the isolated waveforms are graphed in Figure 5a-b. Isolated offset responses synchronized at stimulus offset time with 10 ms pre-offset baseline correction are plotted in Figure 5c. Linear regressions indicate that positive peak latency is significantly correlated ($r^2 = 0.919$, $p < 0.001$), whereas peak amplitude is only weakly correlated ($r^2 = 0.843$, $p = 0.023$), with auditory stimulus duration. Peak amplitude, although arguably giving the appearance of a graded response to stimulus duration, did not achieve the Bonferroni-corrected threshold for statistical significance. Furthermore, these findings were confirmed with rmANOVA. This returned a statistically significant effect of stimulus duration on isolated waveform positive peak latency [$F_{5.13,97.47} = 8.549$, $p = 7.69e^{-7}$; degrees of freedom and p-value corrected with the Greenhouse-Geisser method following violation of Mauchly's test for sphericity]. Also, in this analysis peak amplitude did not reach the threshold for statistical significance [$F_{9,171} = 2.308$, $p = 1.79e^{-2}$; data did not violate Mauchly's test]. Mean offset response peak latency was measured as 23.4 ms (±1.4 ms standard error of the mean; sem) after stimulus offset. This was a slower component than the negative amplitude stimulus-onset peak, which had a mean peak latency of 14.3 ms (±0.5 ms sem) after stimulus onset. No statistically significant effects of sex were observed in these analyses.

4. Discussion

The ERP waveforms in Figure 3 and Figure 4 display a pattern of components comprising N20, P40, and N80 peaks, followed by a slow P200 potential. This depicts a polarity reversal of hippocampal CA3 auditory-evoked local-field-potentials recorded with anterior reference and ground electrodes in previous mouse studies (e.g. Connolly et al., 2004; Siegel et al., 2003). Electrode configuration is known to play a pivotal role in determining ERP morphology; in particular, influencing component polarity (Luck, 2014). For example, mastoid (posterior) versus nasal (anterior) referencing in human EEG studies is known to invert component polarity (Pakarinen et al., 2007). The use of a posterior ground electrode in the present study may therefore be the primary candidate for causing this inversion, although the recording sites being situated in the auditory cortex (dorsal) opposed to the hippocampus (ventral) may also be responsible. Previous studies in rats, recording from the auditory cortex with cerebellar referencing, have shown a pattern of N20, P40, N80 deflections very similar to those observed here from mice (Harms et al., 2014). Overall, this suggests that ERP deflections elicited by auditory stimuli in mice recorded from the hippocampus with anterior referencing are of opposite polarity to those recorded from the cortex with cerebellar referencing. It may be tentatively considered that these reflect common neural generators.

This paper has documented the application of ERP arithmetic to isolate stimulus offset potentials for quantitative analysis, illustrating how this approach may be implemented. The methodological development here is the use of multiple different stimuli ERPs to produce a template to subtract from individual stimuli ERPs in turn to remove gross waveform features, whereas previous approaches have typically relied on subtracting individual stimuli ERPs from one another; e.g. in mismatch negativity studies (Näätänen et al., 2012). To the author's knowledge this is the first time that auditory stimulus offset potentials have been observed from the auditory cortex in conscious mice. Use of instantaneous rise and fall times is likely to have accentuated these, given that fall times are known to influence the magnitude of auditory stimulus-offset responses from the auditory cortex in other small mammals (Qin et al., 2007; Takahashi et al., 2004). Whether these offset responses are present during different amplitude enveloping conditions, and in what form, cannot be ascertained from this data. Comparative analysis of these ERP peaks without performing some procedure to separate them from the gross waveform would have been challenging and possibly introduced a source of subjective bias (e.g. custom baseline corrections and selection of measurement windows for each individual ERP).

Although currently there are no instances of offset potentials being isolated from the ERP found in the literature, it is possible to hypothesize alternative methods for achieving this outcome. For example, in the same manner that eye-blink artefacts are detected and removed from ongoing EEG recordings (Matiko et al., 2013), so it may be possible to mathematically model the larger ERP template, expressly without the offset response, then subtract this to reveal the offset response. It is not immediately clear how the ERP waveform explicitly without the offset response would be modelled without a priori knowledge about its morphology gained through some other method. It may be possible, having now isolated the offset response by ERP arithmetic, to combine its known features with those of the ERP waveform, to computationally isolate offset potentials; however, the motivations for doing so are unobvious. As such, comparisons with alternative methods are limited.

Given that individual ERPs contributed 10% to the average ERP, each may have potentially introduced distortion to the resulting isolated potentials following ERP subtraction. In this case variation between individual ERPs was minimal outside the region of stimulus-offset to stimulus-offset-plus-50 ms. Due to the time-course of offset responses (Figure 5c), and the selection of linearly incremented duration

stimuli (25-275 ms in 25 ms steps), no more than two individual ERPs were deviating substantially from the average (i.e. producing an offset response) at any one time point. This acted to effectively average-out the contributions of individual offset responses from the average ERP. Nevertheless, the relative contribution of each individual ERP must be considered when interpreting waveforms arising from this type of ERP arithmetic, and to determine whether this sort of approach is appropriate for a given data set. The specific operations required may be data-specific, as in this case, but as an example, this data supports the effectiveness of ERP arithmetic as a tool for enhancing the granularity of ERP waveform analysis.

Peak latency and amplitude measurements graphed in Figure 5a-b portray a considerable amount of variation. This is not ideal, although is typically representative of ERP analysis when individual subject data are presented. This may be in large part due to extraneous sources of EMI. This type of variation may be exasperated where a whole-epoch measurement window is applied (e.g. in Figure 5a), although, as mentioned, tuning measurement windows post-hoc introduces subjectivity. Moreover, movement artefacts are extremely difficult to avoid in studies of conscious animals, and also contribute to variation within the data. Notwithstanding this variance, statistical analysis confirmed what is observed by visual inspection of the grand-averaged isolated waveforms; stimuli offset potentials occur in direct response to sound cessation. Given that this methodological approach has revealed a statistically significant result under what may be termed “challenging conditions” for electrophysiology recordings (i.e. recording from conscious mice), it may be equally effective in broader applications with animal or human subjects.

The finding that peak amplitude was not statistically affected by stimulus duration contrasts with previous reports in anaesthetized rats that suggest stimulus duration is an important factor in determining auditory offset response peak amplitude (Takahashi et al., 2004). Perhaps this is because a limited range of stimuli durations (50-275 ms) were employed in the present study; whereas a broader range may have demonstrated the effect of stimulus duration on peak amplitude more clearly. Ambiguity regarding the relationship between peak amplitude and stimulus duration should not detract from the most apparent observation of this study; peak latency is linearly related to auditory stimulus duration. It is thought that the offset response may be caused either by an inhibitory rebound following removal of excitatory auditory input (Takahashi et al., 2004), or a separate process potentially related to duration-tuned neurons (Scholl et al., 2010).

Relatively low amplitudes of offset responses, and difficulty in isolating them, may explain why they have not previously been characterized in conscious rodent ERP studies. Additionally, the acoustic signal-to-noise ratio (SNR; >25 dB), between auditory stimuli and background noise, may have emphasized the offset response, given that on- and off-responses are sensitive to SNR (Baltzell and Billings, 2014). Previous studies in mice where the offset response was not present had SNRs of 5 dB (Maxwell et al., 2004) and 15 dB (Connolly et al., 2004). This information is not always stated in study methods; to facilitate more detailed comparisons across studies, reporting of stimuli intensity and acoustic background noise levels should be encouraged. In auditory neurophysiology experiments, maintaining background acoustic noise levels low is generally preferred when not part of the study design. This aims to mitigate extraneous auditory processing unrelated to the experimental protocol and ensure that low-amplitude peaks, such as offset potentials, are distinguishable.

The method described here may be applied to investigate other instances of time-dependent neurophysiological processing where physical stimuli are applied with a high degree of temporal precision. Visual and tactile modalities are equally applicable in this context, where relative sensory adaptations over time may be examined. This approach is perhaps less likely to be suitable for the study of olfactory or gustatory responses, due to difficulties in controlling the temporal dynamics of

such stimuli (Hummel et al., 2010; Rombaux et al., 2009). Concerning the auditory modality, this approach may find immediate application as a control procedure for duration mismatch negativity studies (Jacobsen and Schröger, 2003). Understanding time-processing in neurological systems, including sensory perceptions, is currently a field of broad scientific interest among the convergent disciplines of psychology, linguistics, and neuroscience (Fontes et al., 2016). This approach of ERP analysis may be applied in these endeavors by aiding to discern and quantify neurophysiological activations occurring at on- and off-set phases of sensory-cognitive events.

In summary, a series of simple arithmetic operations combining multiple stimuli ERPs may be applied to isolate components of interest from the larger amplitude waveform. Specifically, this has led to the identification of stimulus offset potentials recorded from primary auditory cortex of conscious mice. This method may be of particular interest to those investigating time-dependent sensory-cognitive processes.

5. Acknowledgments

I gratefully acknowledge the doctoral supervision of Professors Bernard A. Conway and Judith A. Pratt, and Strathclyde Institute for Pharmacy and Biomedical Sciences for the provision of resources.

6. References

Baltzell, L.S., Billings, C.J., 2014. Sensitivity of offset and onset cortical auditory evoked potentials to signals in noise. Clin. Neurophysiol. 125, 370–380. https://doi.org/10.1016/j.clinph.2013.08.003

Connolly, P.M., Maxwell, C., Liang, Y., Kahn, J.B., Kanes, S.J., Abel, T., Gur, R.E., Turetsky, B.I., Siegel, S.J., 2004. The effects of ketamine vary among inbred mouse strains and mimic schizophrenia for the P80, but not P20 or N40 auditory ERP components. Neurochem. Res. https://doi.org/10.1023/B:NERE.0000023605.68408.fb

Davis, H., Davis, P.A., Loomis, A.L., Harvey, E.N., Hobart, G., 1939. Electrical reactions of the human brain to auditory stimulation during sleep. J. Neurophysiol. 2, 500–514.

Fontes, R., Ribeiro, J., Gupta, D.S., Machado, D., Lopes-Júnior, F., Magalhães, F., Bastos, V.H., Rocha, K., Marinho, V., Lima, G., others, 2016. Time perception mechanisms at central nervous system. Neurol. Int. 8.

Gramfort, A., Luessi, M., Larson, E., Engemann, D.A., Strohmeier, D., Brodbeck, C., Goj, R., Jas, M., Brooks, T., Parkkonen, L., others, 2013. MEG and EEG data analysis with MNE-Python. Front. Neurosci. 7, 267.

Harms, L., Fulham, W.R., Todd, J., Budd, T.W., Hunter, M., Meehan, C., Penttonen, M., Schall, U., Zavitsanou, K., Hodgson, D.M., Michie, P.T., 2014. Mismatch negativity (MMN) in freely-moving rats with several experimental controls. PLoS One 9. https://doi.org/10.1371/journal.pone.0110892

Hummel, T., Genow, A., Landis, B.N., 2010. Clinical assessment of human gustatory function using event related potentials. J. Neurol. Neurosurg. Psychiatry 81, 459–464. https://doi.org/10.1136/jnnp.2009.183699

Ison, J.R., Allen, P.D., O'Neill, W.E., 2007. Age-related hearing loss in C57BL/6J mice has both frequency-specific and non-frequency-specific components that produce a hyperacusis-like exaggeration of the acoustic startle reflex. J. Assoc. Res. Otolaryngol. 8, 539–550.

Jacobsen, T., Schröger, E., 2003. Measuring duration mismatch negativity. Clin. Neurophysiol. 114, 1133–1143. https://doi.org/10.1016/S1388-2457(03)00043-9

Laird, N., Biometrics, J.W.-, 1982, U., n.d. Laird_biometrics_1982.pdf. JSTOR.

Luck, S.J., 2014. An introduction to the event-related potential technique. MIT press.

Luck, S.J., Kappenman, E.S., 2011. The Oxford handbook of event-related potential components. Oxford university press.

Matiko, J.W., Beeby, S., Tudor, J., 2013. Real time eye blink noise removal from EEG signals using morphological component analysis, in: 2013 35th Annual International Conference of the IEEE Engineering in Medicine and Biology Society (EMBC). IEEE, pp. 13–16. https://doi.org/10.1109/EMBC.2013.6609425

Maxwell, C.R., Liang, Y., Weightman, B.D., Kanes, S.J., Abel, T., Gur, R.E., Turetsky, B.I., Bilker, W.B., Lenox, R.H., Siegel, S.J., 2004. Effects of chronic olanzapine and haloperidol differ on the mouse N1 auditory evoked potential. Neuropsychopharmacology. https://doi.org/10.1038/sj.npp.1300376

Näätänen, R., Kujala, T., Escera, C., Baldeweg, T., Kreegipuu, K., Carlson, S., Ponton, C., 2012. The mismatch negativity (MMN)--a unique window to disturbed central auditory processing in

ageing and different clinical conditions. Clin. Neurophysiol. 123, 424–458.

Nakamura, T., Michie, P.T., Fulham, W.R., Todd, J., Budd, T.W., Schall, U., Hunter, M., Hodgson, D.M., 2011. Epidural auditory event-related potentials in the rat to frequency and duration deviants: evidence of mismatch negativity? Front. Psychol. 2, 367.

O'Connor, T.A., Starr, A., 1985. Intracranial potentials correlated with an event-related potential, P300, in the cat.

O'Reilly, J.A., 2018. Oddball and many-standards paradigm auditory-evoked potential data from laboratory mice 1. https://doi.org/10.17632/2V9K8J28VN.1

O'Reilly, J.A., 2017. Characterising mismatch negativity biomarker signatures in preclinical models relevant to schizophrenia. Univ. Strat. Dr. Thesis.

Pakarinen, S., Takegata, R., Rinne, T., Huotilainen, M., Näätänen, R., 2007. Measurement of extensive auditory discrimination profiles using the mismatch negativity (MMN) of the auditory event-related potential (ERP). Clin. Neurophysiol. 118, 177–185.

Paxinos, G., Franklin, K.B.J., 2004. The mouse brain in stereotaxic coordinates.

Qin, L., Chimoto, S., Sakai, M., Wang, J., Sato, Y., 2007. Comparison Between Offset and Onset Responses of Primary Auditory Cortex ON-OFF Neurons in Awake Cats. J. Neurophysiol. 97, 3421–3431. https://doi.org/10.1152/jn.00184.2007

Rombaux, P., Mouraux, A., Collet, S., Eloy, P., Bertrand, B., 2009. Usefulness and feasibility of psychophysical and electrophysiological olfactory testing in the rhinology clinic. Rhinology 47, 28–35. https://doi.org/10.1109/TED.2008.2004475

Ruusuvirta, T., Penttonen, M., Korhonen, T., 1998. Auditory cortical event-related potentials to pitch deviances in rats. Neurosci. Lett. 248, 45–48.

Scholl, B., Gao, X., Wehr, M., 2010. Nonoverlapping sets of synapses drive on responses and off responses in auditory cortex. Neuron 65, 412–421.

Siegel, S.J., Connolly, P., Liang, Y., Lenox, R.H., Gur, R.E., Bilker, W.B., Kanes, S.J., Turetsky, B.I., 2003. Effects of Strain, Novelty and NMDA Blockade on Auditory-Evoked Potentials in Mice. Neuropsychopharmacology 28, 675–682. https://doi.org/10.1038/sj.npp.1300087

Takahashi, H., Nakao, M., Kaga, K., 2004. Cortical mapping of auditory-evoked offset responses in rats. Neuroreport 15, 1565–1569. https://doi.org/10.1097/01.wnr.0000134848.63755.5c

Team, R.C., 2018. R: A Language and Environment for Statistical Computing.

Woodman, G.F., Kang, M.-S., Rossi, A.F., Schall, J.D., 2007. Nonhuman primate event-related potentials indexing covert shifts of attention. Proc. Natl. Acad. Sci. 104, 15111–15116.

8. Figures

Figure 1:

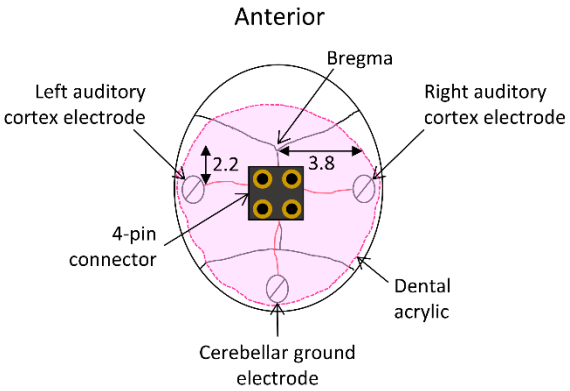

Figure 2:

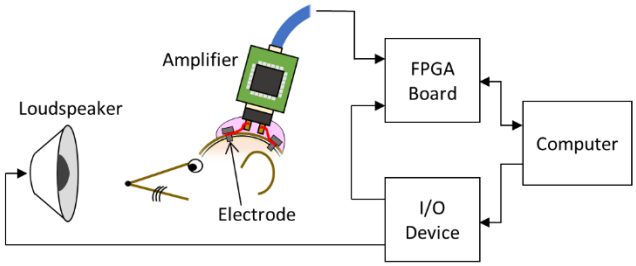

Figure 3:

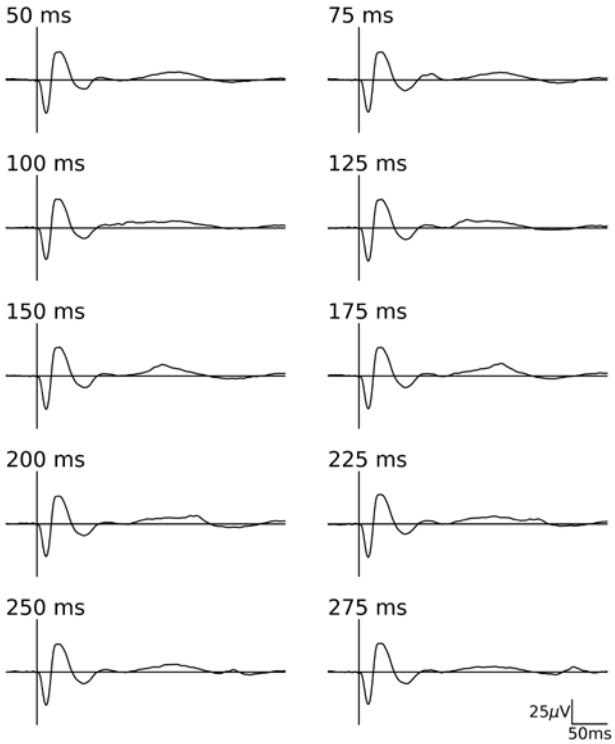

Figure 4:

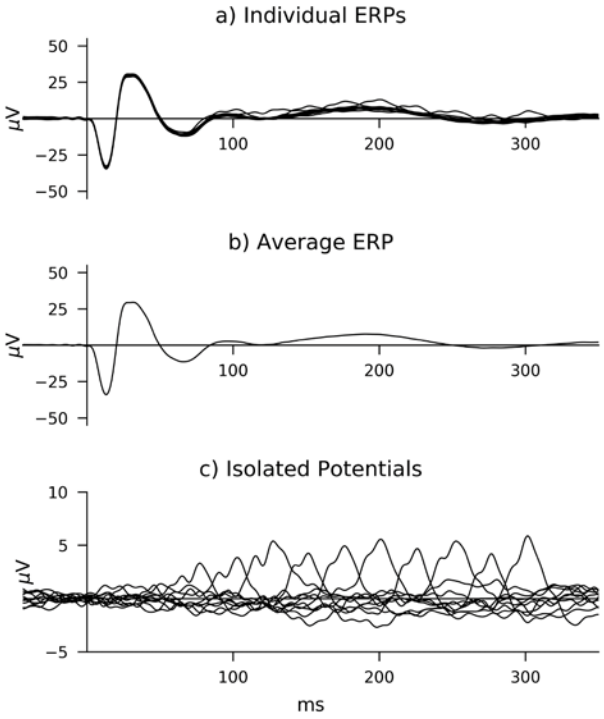

Figure 5:

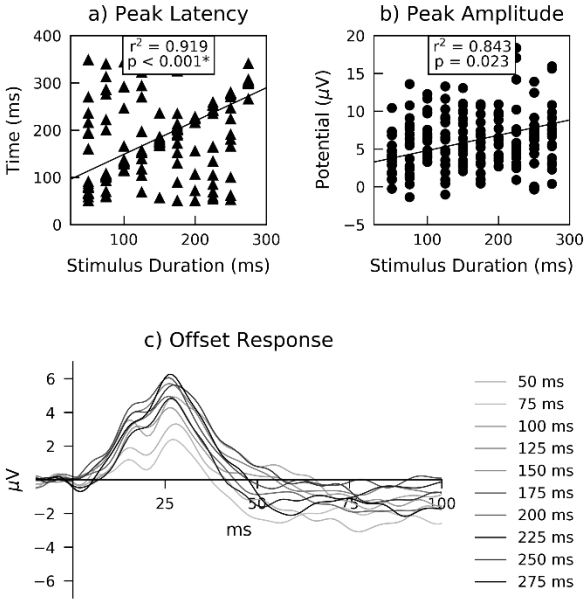

9. Legends

Figure 1: Electrode configuration. Recording electrodes were implanted bilaterally above the primary auditory cortices, with a ground electrode above the cerebellum. These were wired to a connector fixed to the skull using dental acrylic. The ground electrode was bridged across the two posterior connector pins. Measurements relative to Bregma are given in millimeters. This representation is not to scale.

Figure 2: Experiment apparatus. Electrical signals were recorded from the mouse auditory cortex during presentation of sound stimuli, with precise synchronization, for post-hoc analysis of event-related potentials.

Figure 3: Grand-average event-related potential waveforms from ten different duration stimuli. Although there are slight waveform variations, visual inspection of individual ERPs does not necessarily highlight the presence of stimulus-offset effects.

Figure 4: Isolating stimulus offset potentials. a) ERPs from Figure 3 plotted on the same axis. b) The average ERP, produced as in (1). c) The resulting potentials isolated by subtracting the average ERP from each individual ERP (2). This figure illustrates the process of identification and isolation of stimulus offset potentials.

Figure 5: Quantification of isolated potentials. a) Peak latency was found to be significantly correlated with stimulus duration, in agreement with visual observation of the grand-averages. b) Peak amplitude was not found to be significantly correlated with stimulus duration. Linear regression was conducted using the least-squares method. c) Offset response waveforms, plotted with the x-axis relative to stimulus offset time. In (b) and (c) 10 ms pre-offset baseline correction was performed.